Characterization of the nanopore structures of PAN-based carbon fiber precursors by small angle X-ray scattering*

WANG De-Hong(王德红)[1,3] HAO Jun-Jie(郝俊杰)[2,3] XING Xue-Qing(邢雪青)[1,3]
MO Guang(默广)[1] GONG Yu(宫宇)[1,3] LÜ Chun-Xiang(吕春祥)[2] WU Zhong-Hua(吴忠华)[1;1)]

[1] Institute of High Energy Physics, Chinese Academy of Sciences, Beijing 100049, China
[2] Institute of Coal Chemistry, Chinese Academy of Sciences, Taiyuan 030001, China
[3] Graduate University of Chinese Academy of Sciences, Beijing 100049, China

Abstract: The nanopore structures in precursors are crucial to the performance of PAN-based carbon fibers. Four carbon-fiber precursors are prepared. They are bath-fed filaments (A), water-washing filaments (B), hot-stretching filaments (C) and drying-densification filaments (D). Synchrotron radiation small angle X-ray scattering is used to probe and compare the nanopore structures of the four fibers. The nanopore size, discrete volume distribution, nanopore orientation degree along the fiber axis and the porosity are obtained. The results demonstrate that the nanopores are mainly formed in the water-washing stage. During the processes of the subsequent production technologies, the slenderness ratio of nanopores and their orientation degree along the fiber axis increase further and simultaneously, the porosity decreases. These results are helpful for improving the performance of the final carbon fibers.

Key words: PAN-based carbon fiber precursor, small angle X-ray scattering, nanopore structure, porosity

PACS: 61.05.cf, 61.43.Gt **DOI:** 10.1088/1674-1137/35/9/016

1 Introduction

Due to the outstanding mechanical property and smaller specific weight, carbon fibers are widely applied in industrial production. Pursuing the high-performance of carbon fibers is always the motivity for researchers to study them. However, the intrinsic representation of carbon fiber performance is the microstructure, especially the pore structures in carbon fibers. Therefore, the characterization of pore structures in carbon fibers is very important for improving the production technologies and enhancing the production performance. Usually, the formation of carbon fibers includes three main stages: preparation of precursors, pre-oxidation and carbonization. Each stage is possible to cause the formation and change of nanopore's size, distribution and orientation in final carbon fibers. It has been well known that the processes of pre-oxidation and carbonization are relatively complicated and easy to leave a vesicular structure in the final carbon fibers.

In fact, high-quality carbon fibers depend also on high-quality precursors [1]. There have been some open-door reports about the research of carbon fiber precursors [1–3]. A great number of papers have reported the importance of using small angle scattering (SAS) for this purpose [4–11]. Small angle X-ray scattering (SAXS) technique is a powerful tool for characterizing the porosity of materials with pore size ranging from a few Å to about 2000 Å. Besides the high statistic property, SAXS technique is also available to detect the structures of closed pores inside materials, as well as the size, shape and orientation of scatterers so that additional information can be obtained [11]. In this paper, synchrotron radiation SAXS technique is used to probe and compare the nanopore structures

Received 4 December 2010, Revised 13 February 2011
1) Corresponding author. E-mail: wuzh@ihep.ac.cn
* Supported by National Natural Science Foundation of China (10835008), Knowledge Innovation Program of Chinese Academy of Sciences (KJCX3-SYW-N8) and Momentous Equipment Program of Chinese Academy of Sciences (YZ200829)

of four filaments in different stages of forming the polyacrylonitrile (PAN) carbon fibers. It is expected that the results are helpful to improve the production technologies of the resulting carbon fiber.

2 Experiment

Four intermediate filaments in the PAN-based carbon-fiber forming process were prepared at the Institute of Coal Chemistry, the Chinese Academy of Sciences and were marked as sample A, B, C and D respectively. Sample A is bath-fed filaments with the stretching ratio of 1–2. Sample B is water-washing filaments with deionized water of 40–70 ℃; Sample C is hot-stretching filaments with the stretching ratio of 1–1.5 under 70–90 ℃. Sample D is drying-densification filaments after sizing finish.

Synchrotron radiation SAXS measurements were performed at Beamline 1W2A of Beijing Synchrotron Radiation Facility (BSRF). The electron energy of the storage ring is 2.5 GeV and the average current intensity is about 200 mA. The sample-to-detector distance is 1430 mm and the incident X-ray wavelength is 1.54 Å. SAXS patterns of the samples were recorded with a two-dimensional CCD detector with the pixel size of 79 μm. In the SAXS measurements, the scattering patterns of each sample were alternately measured two times at least with the fiber axis of sample parallel to or perpendicular to the horizontal direction, so that the SAXS pattern along the vertical direction on the CCD detector respectively corresponds to the contribution of scatterer sizes perpendicular to the fiber axis or along the fiber axis in the two cases. Using $q=4\ \pi\sin\theta/\lambda$ as the scattering vector, then the detected q-value is from 0.082 to 2.230 nm^{-1}.

3 Data analysis

In the SAXS data analysis, Fit2D software was first used to convert the two dimensional SAXS pattern to one dimensional SAXS curve. In order to distinguish the contribution from the fiber axial direction and the radial direction, the SAXS curve was taken from a strip area across the beam center in vertical direction. By integrating the scattering intensities along the horizontal direction in the strip area, the one dimensional SAXS curve along the vertical direction can be obtained. Because the SAXS intensity around q=0 was commonly absorbed by the beamstop, the smallest and available q-value can not reach q=0. In the following data analysis, the low-q data were complemented by extrapolating the SAXS intensity to q=0 with Guinier plot. Fig. 1 shows the corrected $\ln I \sim q^2$ curves, which respectively correspond to the contribution of scatterer sizes along (the left panel) and perpendicular to (the right panel) the fiber axis. From the SAXS curves, the scatterer sizes and distribution can be obtained. Here, the tangent-by-tangent (TBT) method was used to get the discrete size distribution from $\ln I \sim q^2$ curve [12]. The results are shown in Figs. 2 and 3, respectively, for the pore sizes along the fiber axis or perpendicular to the fiber axis.

Obviously, the average pore size along the fiber axis is larger than that perpendicular to the fiber axis. On the basis of the obtained pore sizes, we assume that the pores in the fibers take an ellipsoidal shape. Therefore, the slenderness ratio (L/D) of an average ellipsoid can be calculated and listed in Table 1. Here, L is the average length and D is the average diameter of such an ellipsoid.

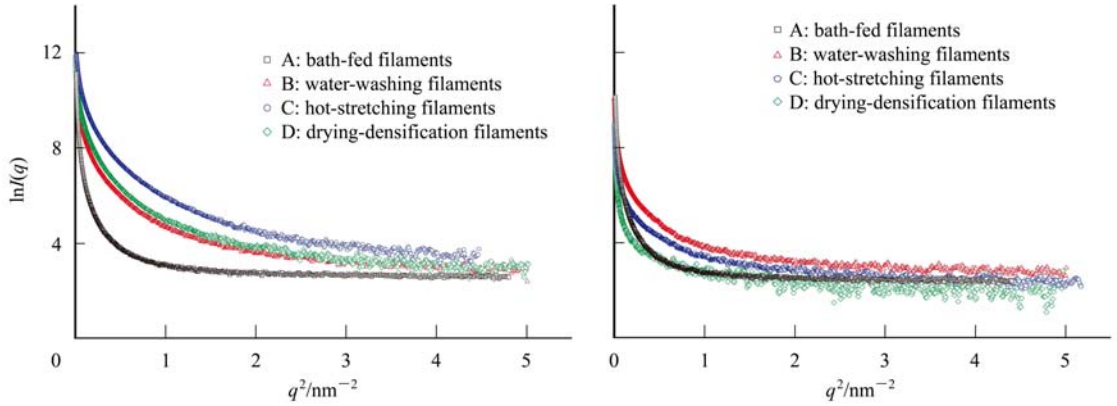

Fig. 1. Guinier plots of small angle X-ray scattering intensities for the four carbon-fiber precursors with the integral strip along the fiber axis (left panel) and perpendicular to the fiber axis (right panel).

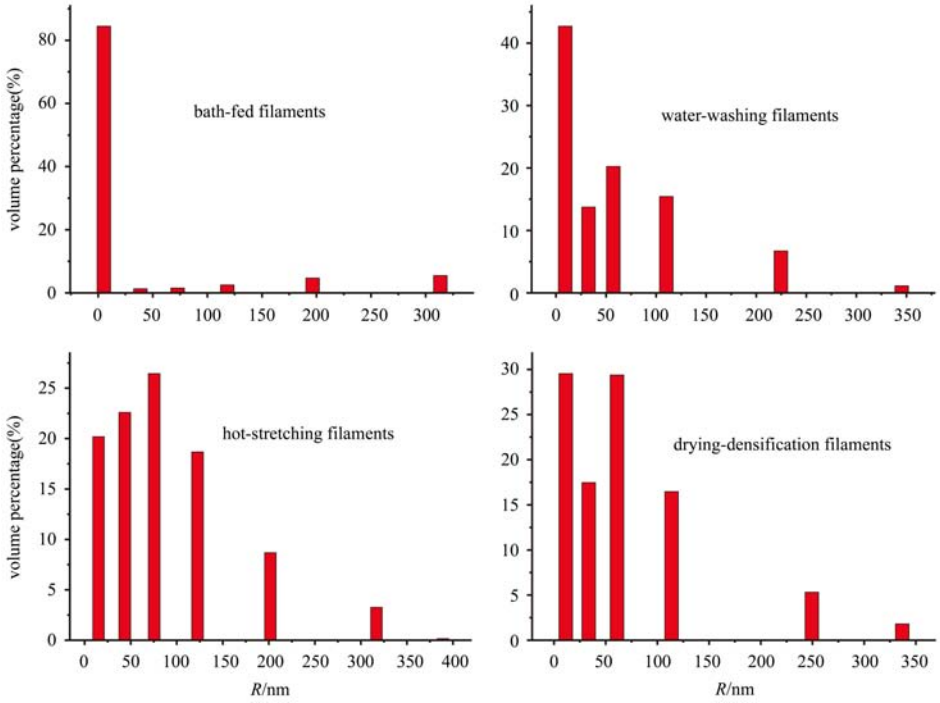

Fig. 2. Discrete distribution of nanopore volumes along the fiber axis direction for the four carbon-fiber precursors.

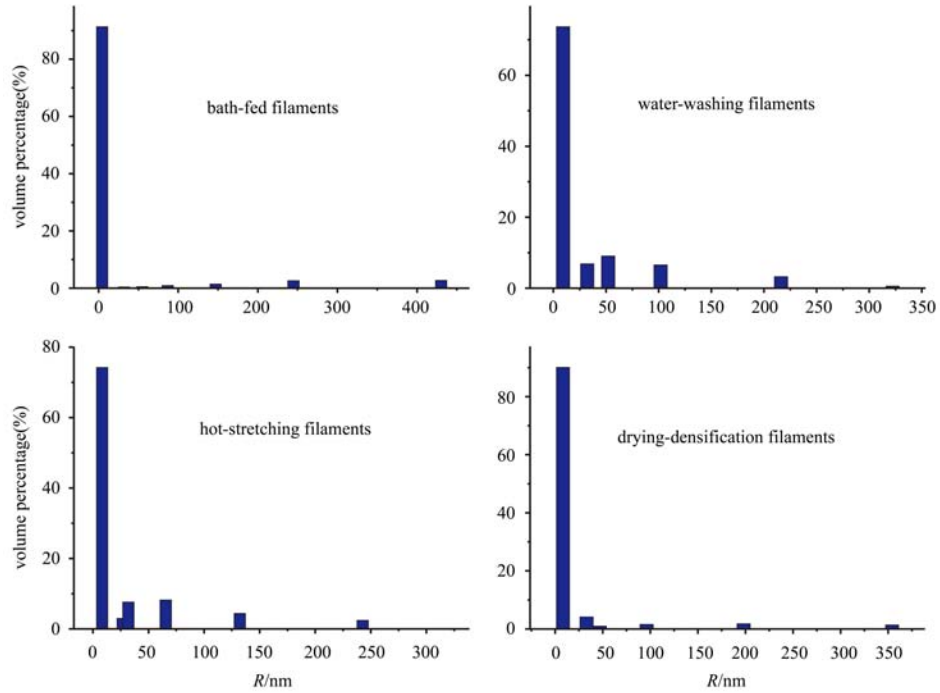

Fig. 3. Discrete distribution of nanopore volumes perpendicular to the fiber axis direction for the four carbon-fiber precursors.

Table 1. Comparison of pore parameters obtained from SAXS for four fibers.

fibers	average length (L)/nm	average diameter (D)/nm	ratio (L/D)	Q_0/Q_{90}	upper limit of porosity(%)
bath-fed filaments	23	16	1.50	0.70	11.7
water-washing filaments	45	20	2.25	0.37	29.4
hot-stretching filaments	48	17	2.84	0.17	21.4
drying-densification filaments	51	15	3.37	0.10	16.9

In order to explore the orientation degree of the ellipsoid pores in the fibers, the Porod's invariant is used to analyze the results acquired with TBT method. For an orientational system with anisotropic scattering elements, the one-dimensional pseudo-invariant Q_α can be defined as [13],

$$Q_\alpha = \int_0^\infty q^2 I_\alpha(q)\mathrm{d}q \tag{1}$$

where α is the angle between the fiber radial direction and the integral-strip direction. With the increase of the orientational degree of the nanopores along the fiber-axis direction, the ratio of Q_0/Q_{90} decreases. By comparing the ratio of Q_0/Q_{90}, the change of orientational degree can be obtained. Here, Q_0 ($\alpha = 0$) is the pseudo-invariant perpendicular to the fiber axis and Q_{90} (α=90) is the pseudo-invariant along the fiber axis. For the four fiber filaments, the acquired orientation degrees are also shown in Table 1.

Another important aspect of the fiber filaments concerning pores is the porosity measurement. Based on the hypothesis of rotation ellipsoidal pores, the porosity of the fiber filaments can be evaluated with the following method.

First, the Porod's length at the α direction can be obtained by using Eq. (2) [14] from the corrected scattering curves taken from α direction.

$$l_{\mathrm{p}\alpha} = \frac{4\int_0^\infty q^2 I_\alpha(q)\mathrm{d}q}{\pi \lim\limits_{q\to\infty} q^4 I_\alpha(q)}. \tag{2}$$

Such a Porod's length is related to the average pore size $\langle l_{\mathrm{pore}}\rangle$ or the average wall size $\langle l_{\mathrm{wall}}\rangle$ by the following formula [15],

$$\frac{1}{l_{\mathrm{p}\alpha}} = \frac{1}{\phi_\alpha \langle l_{\mathrm{wall}}\rangle} = \frac{1}{(1-\phi_\alpha)\langle l_{\mathrm{pore}}\rangle}. \tag{3}$$

where ϕ_α is the porosity along the α direction. $\langle l_{\mathrm{pore}}\rangle$ takes the average value over all possible distances in α direction between pore walls within pores. $\langle l_{\mathrm{wall}}\rangle$ describes an average over all the possible line-lengths connecting two pores in α direction inside the walls of pore [15]. As we know, a particle characteristic length $\langle L\rangle$ can be calculated from the SAXS intensity. For the fiber filaments studied here, the characteristic length $\langle L\rangle$ is taken as the average pore size $\langle l_{\mathrm{pore}}\rangle$ in α direction. Therefore, the pore size $\langle l_{\mathrm{pore}}\rangle$ can be calculated from Eq. (4) [16],

$$\langle l_{\mathrm{pore}}\rangle = \frac{\pi\int_0^\infty q I_\alpha(q)\mathrm{d}q}{\int_0^\infty q^2 I_\alpha(q)\mathrm{d}q}. \tag{4}$$

Combining Eqs. (2)–(4), the porosity can be calculated with the following formula,

$$\phi_\alpha = 1 - \frac{4\left[\int_0^\infty q^2 I_\alpha(q)\mathrm{d}q\right]^2}{\pi^2 \lim\limits_{q\to\infty} q^4 I_\alpha(q)\int_0^\infty q I_\alpha(q)\mathrm{d}q}. \tag{5}$$

Evidently, the porosity obtained with Eq. (5) is not a real porosity because the SAXS intensity along α direction is only considered. But, it is also inappropriate for an anisotropic system to integrate the SAXS intensity along the concentric circle or arc. In this case, the porosity obtained with Eq. (5) is only a projection of global porosity and is defined as the pseudo-porosity here. A sketch map of the integral strip area along α direction is shown in Fig. 4.

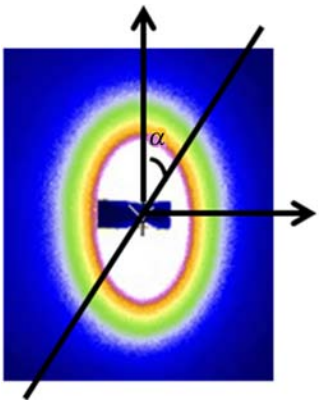

Fig. 4. Sketch map of the integral strip area along α-direction.

As discussed above, the pseudo porosity reflects only a projection of global porosity of the average scatterer with a α-orientation. In fact, the global porosity should be the average over all projective directions (all pseudo porosities). Under the hypothesis that scatterers are rotation ellipsoids, if we have the pseudo porosity ϕ_1 along the fiber axis with α=90 and ϕ_2 perpendicular to the fiber axis with α=0, then the global porosity becomes approximately:

$$P = (\phi_1\phi_2^2)^{1/3} \tag{6}$$

Equation (6) stands for the porosity of the filaments where the pores are equivalent to the rotation ellipsoids with rotation axis along the fiber axis. This porosity is only the upper limit of the real porosity. On the basis of Eq. (6), the global porosities are obtained for the four fiber filaments as shown in Table 1.

4 Results and discussion

The orientation degree of nanopores in the four fiber filaments has been studied with a SAXS tech-

nique. From the discrete pore size distribution, the average pore sizes are obtained. It is found that the average pore size in the bath-fed filaments is generally small, but it increases abruptly when the fibers experience the water-washing process. Then, the average pore size has a gradual change with the subsequent processing technologies. The pore shape becomes more and more elongated. Simultaneously, the orientation degree of nanopores along the fiber axis increases further with the subsequent technologies. This has been confirmed by the ratios of L/D and Q_0/Q_{90} as listed in Table 1. The changes of orientation degree of nanopores are, respectively, obtained with two methods. The orientation tendencies indicated by the ratios of L/D and Q_0/Q_{90} are identical, which demonstrates that the results are reliable.

The porosities in the fiber filaments have also been analyzed. The results demonstrate that the porosity increases suddenly in the water-washing stage. This is in agreement with the change of slenderness ratio of nanopores. With the progress of the subsequent manufacturing procedure, the porosity is gradually decreased. For example, the porosity in the hot-stretching filaments has decreased to 21.4%. In drying densification step, the orientation degree of the nonspherical nanopores becomes further higher with L/D ratio of 3.47 and the porosity decreases further to 16.9%. This is because a stretching force is applied to the fiber axial direction in these subsequent technologies, resulting in an increase of the slenderness ratio of the nanopores and the decrease of their average volume. The decrease of porosity is good for the increase of the fiber strength.

Combining the results of pore sizes, slenderness ratio and porosity, we think that the water-washing technology is a crucial process. In the water-washing stage, both increases of the pore size and the porosity will result in the decrease of performance of the resulting carbon fibers. In our case, the average pore size reaches up to 45 nm (along the fiber axis) and 20 nm (perpendicular to the fiber axis) in the water-washing filaments. The porosity is also up to 29.4%. A possible reason is that some solvents remained in the nascent fibers. When the nascent fibers were water-washed, these solvent residues were washed down and left the channels, thus forming open pores in the surface of fibers. Therefore, controlling the amount of residues absorbed in the nascent fibers is helpful for the performance of carbon fibers.

5 Conclusions

Synchrotron radiation SAXS technique is used to probe the nanopore structures of PAN-based carbon fiber precursors. The pore size, pore size distribution, orientation degree and the porosity are obtained. The results demonstrate that the nanopores are mainly formed in the water-washing stage. Controlling the amount of residues absorbed in the nascent fibers is helpful to the improvement of carbon fiber performance. The subsequent technologies in the production of carbon fibers make the nanopore size decrease, the nanopore orientation degree increasie and the porosity decrease.

References

1 SUN Jin-Feng, CHEN Jie, LIU Wei-Ling, ZHU Wei-Ping, WU Yong-Xing. Hi-Tech Fiber & Application, 2006, **31**(2): 38 (in Chinese)
2 WANG Yan-Xiang, WANG Cheng-Guo, DONG Xue-Mei, HE Dong-Xin. Petrochemical Technology in Jinshan, 2002, **21**(4): 5 (in Chinese)
3 QI Zhi-Jun, SONG Wei, LIN Shu-Bo. Hi-Tech Fiber & Application, 2001, **26**(5): 18 (in Chinese)
4 Foster M D, Jensen K F. Carbon, 1991, **29**(2): 271
5 Gupta A, Harrison I R. Carbon, 1994, **32**(5): 953
6 Nakagawa T, Nishikawa K, Komaki I. Carbon, 1999, **37**(3): 520
7 LI X K, LIU L, LI Z H, WU D, SHEN S D. Carbon, 2000, **38**(4): 623
8 Diduszko R, Swiatkowski A, Trznadel B J. Carbon, 2000, **38**(8): 1153
9 Hall P J, Brown S, Fernández J, Calo J M. Carbon, 2000, **38**(8): 1257
10 Cohaut N, Blanche C, Dumas D, Guet J M, Rouzaud J N. Carbon, 2000, **38**(9): 1391
11 Cazorla-Amoros D, Salinas-Martinez de Lecea C, Alcaniz-Monge J, Gardner M, North A, Dore J. Carbon, 1998, **36**(4): 309
12 WANG Wei, CHEN Xing, CAI Quan, MO Guang, CHEN Zhong-Jun, LI Zhi-Hong, ZHANG Kun-Hao, WU Zhong-Hua. Nuclear Techniques, 2007, **30**(7): 571 (in Chinese)
13 Effler L J, Fellers J F. Journal of Physics D: Applied Physics. 1992, **25**(1): 74
14 Perret R, Ruland W. Kolloid-Zeitschrift und Zeitschrift fur Polymere, 1971, **247**(1): 835
15 Weber J, Bergstrom L. Langmuir, 2010, **26**(12): 10158
16 MENG Zhao-Fu. Small Angle X-Ray Scattering Theory and Application. Jilin: Jilin Science and Technology Publisher, 1996. 68 (in Chinese)